International Journal of Smart Home
Vol. 9, No. 12, (2015), pp. 255-266
http://dx.doi.org/10.14257/ijsh.2015.9.12.26

A Low-cost IMU/GNSS Cooperative Positioning Method for VANETs in the Urban Environments

Yong Hao and Feng Shen

College of Automation, Harbin Engineering University, Harbin, China
sf407@126.com

Abstract

It is important to know the key problem of the emerging intelligent transportation systems –relative position, especially in the collision warning and speeds advisory. However, the commercial Global Satellite Navigation Systems (GNSS) receiver cannot up to the standard of these purpose. Fortunately, using Cooperative Positioning (CP) techniques to share the GNSS measurements between vehicles can largely improve the performance of relative positioning in a vehicular ad hoc network (VANET). But in urban environments, the reduced quality or complete unavailability of GNSS measurements challenge the effectiveness of any CP algorithm. In this paper, a new improved tight CP technique is proposed which adds the measurements from low cost inertial sensors. In the enhanced CP method proposed here, vehicles communicate their GPS measurements and inertial measurement unit (IMU) data, and each vehicle fuses local GPS and IMU measurements and those of the neighbours. Experimental results show that the new tight integration CP method can enhance the relative positioning in low GPS coverage environment, such as in very dense urban areas and tunnels.

Keywords*: Cooperative Positioning, GNSS, inertial navigation sensors, tight integration, vehicular ad hoc network.*

1. Introduction

Relative position-aware is a key factor for many applications such as intelligent transportation systems (ITS) and location based services (LBS) [1] [2]. As one of the ways of position obtaining, Global Navigation Satellite Systems (GNSS) is widely used in intelligent transportation systems. Unfortunately, current commercially available GNSS receivers suffers the positioning error up to tens of meters, which can not satisfy some safety-critical applications, such as collision avoidance and lane-level guidance. Today, the improvement in wireless networks encourage the enhance of Cooperative Positioning (CP) technology in vehicular ad hoc networks (VANETs) [3-5]. The performance of absolute positioning and relative positioning can be improved by CP technology, which combine the measurements among the vehicles.)

So far, several Cooperative Positioning techniques have been proposed to improve positioning performance. Some typical CP techniques are real-time kinematic (RTK) [6], satellite/ground-based augmentation systems [7], and differential GPS (DGPS) [8]. However, those techniques rely on the infrastructure and can not do well enough in urban environments because of the limited vision, non-line-of-sight and multipath problems from those near tall buildings. Recently, many CP techniques, via vehicle-vehicle communication, are raised to overcome these problems, which gain the relative / absolute position through breaking the range and GNSS measurements [9]-[12]. Nevertheless, these techniques rely on radio-based ranging methods, such as time of arrival (TOA), time difference of arrival (TDOA), angle of arrival (AOA), and received signal strength (RSS),

ISSN: 1975-4094 IJSH

which normally require particular sensors with high computational complexity and/or suffer from inadequate ranging accuracy. Based on ranging-rate，some other CP approaches are proposed to avoid the complexities of range-based CP methods [13]-[15]. However, the relative velocity among vehicles have significant influence on the performance of ranging-rate-based CP approaches. As shown in [15], when the relative velocity is lower than 20 km/h, the range-rate-based CP methods have little improvement, which are not suitable for dense urban environments. For accepting double differencing principles, the tight combination CP technique was proposed in [16], and it did not need any range or ranging-rate information. Meanwhile, this method eliminates the infrastructure costs and attains greater implement in position relative compared with DGPS. Furthermore, [17] proposed an tight integration way aiding with INS for purpose of relative positioning, and it has 10% and 35% improvement over tightly coupled CP in full GPS coverage or complete GPS outage environments, respectively. However, further experimentation with the method in [17] shows that the improvements of the GNSS outage leads to the decrease of the performance in regard to DGPS. This is especially true when the length of time of GPS break off is more than 12 seconds using the dataset in [17], the performance of tightly combine way aiding by INS, in terms of relative positioning accuracy, is observed to be worse than tight integration CP and DGPS. In this paper, we propose a new IMU/GPS tight integration CP method that targets performance improvements in GPS low coverage environments, such as very dense urban areas. In this method, besides GPS pseudoranges and GPS Doppler shifts, the acceleration of the vehicle calculated by the IMU is also shared among the participating vehicles. Experimental results show that, in the simulation dense urban scenario, the proposed method has up to 23%, 26%, and 33% improvement, in terms of *rmse*, over the INS-aided tight CP [17], the tight CP [16] and DGPS [7], respectively. In the extremely abominable environment, GPS complete outage, up to 35%, 45%, and 54% improvement, were achieved over the tight CP aided with INS, the tight CP and DGPS, respectively.

The remainder of this paper is organized as follows. In section II, the problem and solution approach are explained. Section III details the estimator of the proposed CP method. In section IV the experimental results are discussed, and the performance of the proposed system is evaluated. Section V summarizes the contributions of this work.

2. Problem Definition and Solution Design

The main problem of this paper attempts to address is to find a low cost IMU-aided tight CP solution to improve the relative position precision in GPS low coverage area, such as in very dense urban areas and tunnels. And in the proposed CP solution, we assumes that each participating vehicle is equipped with GPS receivers and low cost IMUs and can communicate to share their data, such as pseudoranges and Doppler shifts from GPS receivers, the accelerations from IMUs. Both full GPS signal coverage and low GPS signal coverage is considered in the analysis. The ultimate goal of the proposed method is that each vehicle can improve precision of its position relative to its neighbours using a data fusion algorithm, which is fed by local GPS and IMU measurements and those of the neighbours.

2.1 Classic Double Difference Pseudorange Solution

The pseudorange (distance between satellite and vehicle) is calculated from the signal transmission time. There are many sources can result in the errors of the pseudorange measurements. Particularly, the pseudorange observable between satellite i and receiver k at time t, which is denoted $\rho_k^i(t)$, can be defined as [18]

$$\rho_k^i(t) = R_k^i(t) + \delta_k(t) + d^i + \zeta_k^i(t) \tag{1}$$

where R_k^i is the real distance between satellite i and the vehicle k, and d^i is the general noise correlated to the satellite i, which includes atmospheric delay, satellite bias, and the

ephemeris errors, and δ_k is the distance error results from the receiver k 's clock error , ζ_k^i is the non-shared noise correlated to both satellite i and receiver k, which includes multipath noise and thermal noise.

We can eliminate the common noise caused by the satellite i through taking the single differencing between the pseudoranges of two receivers k and l to the same satellite i as follows.The clock bias k and l can be eliminated through using the double differencing technique, if the receivers can receive both the signal from satellite i and j. We can get the pseudoranges as follows:

$$\rho_{kl}^{ij}(t) = R_{kl}^{ij}(t) + \zeta_{kl}^{ij}(t) \tag{2}$$

where ζ_{kl}^{ij} is the remnant of uncorrelated errors which can not be eliminated through double differencing, and $R_{kl}^{ij}(t)$ is the double difference of the true ranges between the receivers and satellites, which can be described as

$$R_{kl}^{ij}(t) = [\vec{u}_i(t) - \vec{u}_j(t)]^T \vec{r}_{kl}(t) \tag{3}$$

where, $\vec{u}_i$ and $\vec{u}_j$ are the unitized vector which points from receiver k to the satellite i and j. $\vec{r}_{kl}$ is the distance vector between receiver k and receiver l.

So, we can redescribe the double differences of the GPS pseudoranges as follow:

$$\rho_{kl}^{ij}(t) = [\vec{u}_i(t) - \vec{u}_j(t)]^T \vec{r}_{kl}(t) + \zeta_{kl}^{ij}(t) \tag{4}$$

It can be seen that, while calculating the unit vector of $\vec{u}_i$ or $\vec{u}_j$, the positioning error of the GPS can be overlooked because of the distance between the satellites and the GPS receivers is about 20 000 km, which is much larger than the error. As a consequence, we can calculate the $\vec{u}_i$ and $\vec{u}_j$ through the corresponding ephemeris and the GPS fixes [19].

We use the GPS Doppler shifts in the proposed tight CP technique. From equation (4), the double differences of GPS Doppler shifts for receiver k and l and satellites i and j, which is denoted $\vartheta_{kl}^{ij}(t)$, can be deduced as [17]

$$\vartheta_{kl}^{ij}(t) = \frac{1}{\lambda}[\vec{u}_i(t) - \vec{u}_j(t)]^T \vec{v}_{kl}(t) + \gamma_{kl}^{ij}(t) \tag{5}$$

where, $\vec{v}_{kl}$ is the relative velocity between vehicles k and l, and λ is the wavelength of the GPS L1 signal and $\gamma_{kl}^{ij}(t)$ is observation noise.

2.2 Low Cost IMU-Aided Tight CP Approach

In the tight CP method used to be, the accelerations of vehicles, which are obtained from IMU, will share between vehicles and fuse with the GPS measurements together.

Inertial units have always been presented as a valuable sensor in many applications [20]. A typical IMU consists of three accelerometers and three gyroscopes mounted in a set of three orthogonal axes, called body frame. The IMU measures the acceleration and the rotation rate of the vehicle along the three axes of the body frame. Fig. 1 shows a vehicle moving on the earth surface. The Navigation frame n represented by the orthogonal axis East-North-Up (ENU) is the coordinate frame with respect to which the location of the vehicle needs to be estimated. For inertial navigation, the Euler angles, i.e., roll (φ), pitch (θ), and yaw (ψ), are used. The roll, pitch, and yaw are the angles that the body frame should rotate around three orthogonal axes X, Y, and Z of body frame, respectively, to align with the axes of the navigation frame. C_b^n is the rotation matrix that is defined based on the Euler angles to align the body frame to the navigation frame, which can be expressed as [21]

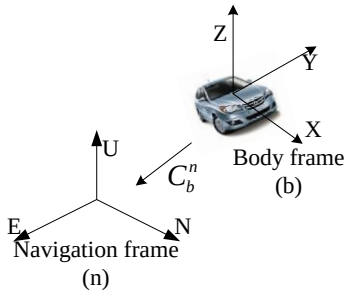

Figure 1. Motion of a Vehicle on a Surface

$$C_b^n = \begin{bmatrix} \psi_c\theta_c & \psi_c\theta_s\varphi_s - \psi_s\varphi_c & \psi_c\theta_s\varphi_c + \psi_s\varphi_s \\ \psi_s\theta_c & \psi_s\theta_s\varphi_s + \psi_c\varphi_c & \psi_s\theta_s\varphi_c - \psi_c\varphi_s \\ -\theta_s & \theta_c\varphi_s & \theta_c\varphi_c \end{bmatrix} \tag{6}$$

where we subscript sine and cosine as s and c . Equation (6) is well known in inertial navigation theory, and more details on the derivation of rotation matrix can be found in [21]. According to [21], the motion of a vehicle can be modelled as

$$\dot{\vec{P}}_n = \vec{V}_n \tag{7}$$

$$\ddot{\vec{P}}_n = \dot{\vec{V}}_n = \vec{a}_n = C_b^n \vec{a}_b - \vec{g} \tag{8}$$

where subscripts n and b refer to navigation frame and body frame, respectively, $\vec{p}_n$ is the position vector of the vehicle, $\vec{v}_n$ is the velocity vector of the vehicle, $\vec{g}$ is the earth gravity vector, and $\vec{a}$ is the acceleration vector where the description n and b represent navigation frame and body frame, respectively. Note that the acceleration measurements from the IMU are represented by $\vec{a}_n$. For simplicity, we will use $\vec{a}$ to represent $\vec{a}_n$ in the rest of this paper. For the ENU coordinate system $\vec{g}$ is a vector with zero entries for the East and North elements, and earth gravity $g \approx -9.8 / s^2$.

To enhance the tight CP in this paper, the observations of relative acceleration between vehicles k and l are used. Define $\vec{a}_{kl} = \vec{a}_l - \vec{a}_k$ as relative acceleration, where $\vec{a}_l, \vec{a}_k$ are the acceleration vectors $\vec{a}$ of vehicle k and l, and then the relative acceleration can be calculated as

$$\vec{a}_{kl} = C_{bl}^n \vec{a}_{bl} - C_{bk}^n \vec{a}_{bk} \tag{9}$$

According to (9), $\vec{a}$ can be calculated using $\vec{a}_b$ that is measured by IMU accelerometers and C_b^n that is calculated based on the Euler angles. The Euler angles $[\theta \quad \varphi \quad \psi]^{\mathrm{T}}$ can be updated using the rotation rate provided by the gyro of the IMU $[\omega_{bx} \quad \omega_{by} \quad \omega_{bz}]^{\mathrm{T}}$ as follows [21].

$$\dot{\psi} = [\omega_{by} \sin\varphi + \omega_{bz} \cos\varphi]\cos(\theta)^{-1} \tag{10}$$

$$\dot{\theta} = \omega_{by} \cos\varphi - \omega_{bz} \sin\varphi \tag{11}$$

$$\dot{\varphi} = \omega_{bx} + [\omega_{by} \sin\varphi + \omega_{bz} \cos\varphi]\tan(\theta) \tag{12}$$

3. The Solution of Tight CP

In this section we will present the tight integration CP method we proposed, with the measurements have all defined. Fig. 2 show us the structure of tight integration CP. In this method, three measurements, GPS pseudoranges and GPS Doppler shifts and accelerations, are all shared among vehicles. Then the local GPS pseudoranges and GPS Doppler shifts are double differenced with the received pseudoranges and Doppler shifts to get the double difference measurements as shown in (4) and (5), and the local accelerations are differenced with the received accelerations to obtain the relative accelerations as shown in (9). The differencing of the received and local measurements' process is realized in our Tight CP Kalman Filter as shown in the Fig. 2. It is worth noting that, with the GPS full coverage, a GPS receiver can be used for the IMU alignment, which is not the emphasis of this paper. For details about alignment methods, refer to [22] and [23].

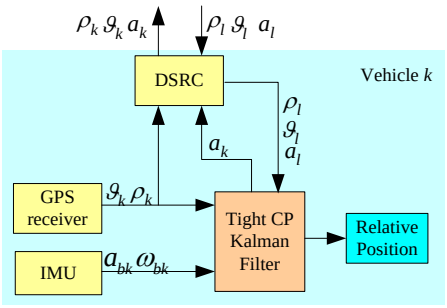

Figure 2. Tight Integration CP Architecture

A Kalman filter is used in tight CP to fuse the available sensors for relative positioning. In this paper, we modify the Euler updating equations to be used in the linear Kalman filter. We adopt $[x_1 \quad x_2 \quad x_3]^{\mathrm{T}}$ instead of $[\theta \quad \varphi \quad \psi]^{\mathrm{T}}$ as the state variables, where,

$$x_1 = -\sin\theta \tag{13}$$

$$x_2 = \sin\varphi\cos\theta \tag{14}$$

$$x_3 = \cos\varphi\cos\theta \tag{15}$$

Substituting the equations (11) and (12) in (13), (14) and (15) yields:

$$\dot{x}_1 = -\dot{\theta}\cos\theta = \omega_{bz}x_2 - \omega_{by}x_3 \tag{16}$$

$$\dot{x}_2 = \dot{\varphi}\cos\varphi\cos\theta - \dot{\theta}\sin\varphi\sin\theta = -\omega_{bz}x_1 + \omega_{bx}x_3 \tag{17}$$

$$\dot{x}_3 = -\dot{\varphi}\sin\varphi\cos\theta - \dot{\theta}\cos\varphi\sin\theta = \omega_{by}x_1 - \omega_{bx}x_2 \tag{18}$$

Equations (16) – (18) represents the second part the state transformation matrix to be used in the Kalman filter as will be seen in equation (25).

As part of the input to the Kalman filter, the rotation matrix C_b^n needs to be provided. To obtain this, it is first noted that the derivative of the yaw angle $\dot{\psi}$ in equation (10) can be transformed to

$$\dot{\psi} = \frac{x_2}{x_2^2 + x_3^2}\omega_{by} + \frac{x_3}{x_2^2 + x_3^2}\omega_{bz} \tag{19}$$

Therefore, the yaw angle ψ can be obtained by integrating equation (19). Similarly, the roll (φ) and pitch (θ) can be calculated directly through (13)-(15). The result of inferring the Euler angles via equations (13)-(15) is crucial in determining the values of the rotation matrix C_b^n that depends on the Euler angles $[\theta \quad \varphi \quad \psi]^{\mathrm{T}}$.

The system model of proposed Kalman filter-based tight CP is defined as

$$X(t+\tau) = FX(t) + GW(t) \tag{20}$$

where X is the state vector, F is the state transition model, G is the process noise model, W is the noise vector, and τ is the observation period. The system states can be divided into two parts, the first part consists of the relative position, velocity and acceleration, and the second part is the Euler angles. So (20) can be reformulated as

$$\begin{bmatrix} X_1(t+\tau) \\ X_2(t+\tau) \end{bmatrix} = \begin{bmatrix} F_1 & F_3 \\ F_4 & F_2 \end{bmatrix} \begin{bmatrix} X_1(t) \\ X_2(t) \end{bmatrix} + \begin{bmatrix} G_1 & G_3 \\ G_4 & G_2 \end{bmatrix} \begin{bmatrix} W_1(t) \\ W_2(t) \end{bmatrix} \tag{21}$$

The matrices and state variables of vehicle l with respect to vehicle k are defined as

$$X_1 = [\vec{r}_{kl} \ \ \vec{v}_{kl} \ \ \vec{a}_{kl} \ ]^T \tag{22}$$

$$X_2 = [x_1 \ x_2 \ x_3]^T \tag{23}$$

$$F_1 = \begin{bmatrix} I_3 & \tau I_3 & 0.5\tau^2 I_3 \\ 0_3 & I_3 & \tau I_3 \\ 0_3 & 0_3 & I_3 \end{bmatrix} \tag{24}$$

$$F_2 = \begin{bmatrix} 0 & \omega_{bz} & -\omega_{by} \\ -\omega_{bz} & 0 & \omega_{bx} \\ \omega_{by} & -\omega_{bx} & 0 \end{bmatrix} \tag{25}$$

$$F_3 = [0_{9\times 3}] \tag{26}$$

$$F_4 = [0_{3\times 9}] \tag{27}$$

$$G_1 = [0.5\tau^2 I_3 \ \ \tau I_3 \ \ I_3]^T \tag{28}$$

$$G_2 = \begin{bmatrix} 0 & x_3 & -x_2 \\ -x_3 & 0 & x_1 \\ x_2 & -x_1 & 0 \end{bmatrix} \tag{29}$$

$$G_3 = [0_{9\times 3}], \ G_4 = [0_{3\times 3}] \tag{30}$$

where $0_{m\times n}$ is an $m \times n$ matrix with all zero entries, and I_n is an identity matrix with size n. Assume $W_1(t)$ is the Gaussian relative acceleration noise with standard deviation σ and zero mean along each axis, and then the covariance of $W_1(t)$, i.e., Q1, is $Q_1 = \sigma_\varsigma^2 G_1 G_1^T$, $W_2(t)$ is Euler angle noise with the covariance $Q_2 = 2\sigma_{bia}^2 G_2$, whose values are obtained from Allan Variance analysis on static IMU data. The details of static error analysis using Allan Variance is not the emphasis in this paper, but can be found in [22]. Then the covariance of process noise, i.e., Q, is

$$Q = \begin{bmatrix} Q_1 & 0_{9\times 3} \\ 0_{3\times 9} & Q_2 \end{bmatrix} \tag{31}$$

The observation model of proposed tight CP system is

$$Z(t) = H(t)X(t) + \zeta(t) \tag{32}$$

Where Z is the observation vector, H is the observation model, and ζ is the observation noise. In the proposed method, the double differences of the GPS pseudoranges and Doppler shifts and the relative acceleration, i.e., (4), (5), and (9), are used as the observation vector which is defined as follows,

$$Z = \begin{bmatrix} \rho_{kl}^{12} & \cdots & \rho_{kl}^{1m} & \vartheta_{kl}^{12} & \cdots & \vartheta_{kl}^{12} & \vec{a}_{kl}^{T} \end{bmatrix}^{T} \tag{33}$$

$$\zeta = \begin{bmatrix} \zeta_{kl}^{12} & \cdots & \zeta_{kl}^{1m} & \gamma_{kl}^{12} & \cdots & \gamma_{kl}^{12} & \vec{\delta}_{kl}^{T} \end{bmatrix}^{T} \tag{34}$$

where $\vec{\delta}_{kl}$ is the IMU acceleration noise with the covariance σ_a^2 , and is independent among three axes. m is the number of common GPS satellites visible at vehicles k and l. We choose the satellite with the highest elevation angle. According to (4), (5), (9), and (16)-(18), we have

$$H = \begin{bmatrix} U & 0_{(m-1)\times 3} & 0_{(m-1)\times 3} & 0_{(m-1)\times 3} \\ 0_{(m-1)\times 3} & -U\lambda^{-1} & 0_{(m-1)\times 3} & 0_{(m-1)\times 3} \\ 0_3 & 0_3 & I_3 & 0_3 \end{bmatrix} \tag{35}$$

where

$$U(t) = \begin{bmatrix} \vec{u}_1^{T}(t) - \vec{u}_2^{T}(t) \\ \vec{u}_1^{T}(t) - \vec{u}_3^{T}(t) \\ \vdots \\ \vec{u}_1^{T}(t) - \vec{u}_m^{T}(t) \end{bmatrix} \tag{36}$$

Assuming that observations are independent, then the observation noise covariance can be expressed as

$$\Sigma = \begin{bmatrix} \Sigma_\rho & 0_{m-1} & 0_{(m-1)\times 3} \\ 0_{m-1} & \Sigma_\vartheta & 0_{(m-1)\times 3} \\ 0_{(m-1)\times 3}{}^{T} & 0_{(m-1)\times 3}{}^{T} & \Sigma_a \end{bmatrix} \tag{37}$$

Considering that the rotational matrix C_b^n is orthogonal, the covariance of the acceleration noise for the navigation frame will also be $\sigma_a^2 I_3$. Therefore, the covariance of relative acceleration is $\Sigma_a = 2\sigma_a^2 I_3$. Defining σ_p^2 and σ_ϑ^2 as the variance of the GPS pseudorange and the Doppler shift observation error, respectively we have [17] $\Sigma_\rho = \sigma_\rho^2 AA^T$ and $\Sigma_\vartheta = \sigma_\vartheta^2 AA^T$, where

$$A = \begin{bmatrix} 1_{(m-1)\times 1} & -I_{(m-1)} & -1_{(m-1)\times 1} & I_{(m-1)} \end{bmatrix} \tag{38}$$

The tight CP now is completed with the above description.

4. Experimental Results

The experiment data is used to calculate the presented tight CP methods. We used to use two vehicles which contain GPS receivers and INSs. One of the vehicles equipped with expensive reference equipment, and another equipped with low cost sensors. The reference equipment is the Leica GS10 receiver for vehicle 1, and a Novatel INS-LCI (integrated GNSS-INS) for vehicle 2. We can use receivers' carrier-phase-based differential position estimates (RTK) as the ground truth position data. The measurements of the tight CP algorithm are the Doppler shifts, the noisy L1 pseudoranges , and the low-cost MEMS IMU.

More than 14 minutes data were selected of the whole experiment. We use GPS observations to calculate the DGPS corrections.)The test area was Clifton Boulevard, between Derby Road and Loughborough Road in Nottingham, U.K., and it has good open sky to maximize satellite visibility. The Dedicated Short Range Communications (DSRC) supplied by University of New South Wales (UNSW) is used for vehicular communication with 75-MHz bandwidth at 5.9 GHz. Some details about DSRC can be found in [10] and [25]， it is concluded that the bandwidth of DSRC is far beyond the requirements of tight CP [16]. Therefore, even adding a few bytes for IMU data in the proposed CP algorithm, the

bandwidth of DSRC is not a concern because the considered broadcast data needs a bandwidth much lower than the bandwidth of DSRC channels, 10 MHz, even if the update rate is a few per second.

The performance of DGPS [7], the tight CP method proposed in [16], the INS-aided tight CP method proposed in [17], and the low-cost IMU tight CP method proposed here are compared using the same experimental data. To describe conveniently, "DGPS", "T-CP", "INS-aided T-CP" and "T-CP with IMU" are used in the following figures and table to denote the four methods mentioned above. The two vehicles' relative distance errors, i.e., $e_d(t) = |\vec{r}'(t) - \vec{r}(t)|$, was estimated, where $\vec{r}'(t)$ and $\vec{r}(t)$ are the estimated relative position and the true relative position respectively.

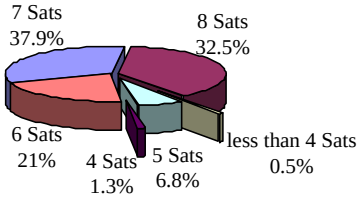

Figure 3. Common Satellite Visibility of the Experimental Data Selected

Fig. 3 shows the common satellite visibility at two vehicles of the experimental data selected. As can be seen that, the number of common satellite in the most of observation time is more than 5. Firstly, we use this scenario as full GPS coverage to evaluate the performance of proposed method. Table 1 summarizes the performance indicators for the experimental results. It can be known that the low-cost IMU tight CP method used in this paper is better than the DGPS and tight CP method, and has similar performance to the INS-aided tight CP method.

Table 1. Experimental Results for Relative Positioning Errors

Methods	rmse (m)	accuracy(m)	Precision(m)
T-CP with IMU (proposed)	1.74	1.39	1.04
INS-aided T-CP [17]	1.75	1.40	1.05
T-CP [16]	1.84	1.42	1.17
DGPS [7]	2.05	1.52	1.38

As mentioned previously, the purpose of the proposed CP method in this paper is to improve the CP performance in the dense urban environment, where the GPS is low coverage and outage frequency. To simulate urban environment, we use the experimental results investigated by J. Chao et al [26] in Hong Kong districts, which showed that the number of visible satellite were no more than 6 in the most of observation time. Therefore, to further evaluate the performance of the proposed method in dense urban environment, we manually masked two GPS satellites of the select data to emulate obstructions to low elevation satellites, which is more representative of dense urban scenarios. Fig. 4 shows the common satellites visibility simulation of dense urban scenarios, where in about 30% of total observation time the number of visible satellite is no more than 4.

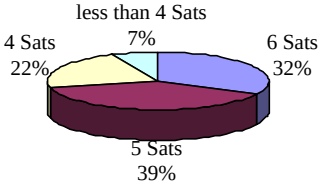

Figure 4. The Common Satellites Visibility Simulation for Dense Urban Scenarios

Table 2 summarizes the performance indicators for the experimental results in the simulation dense urban scenarios. As can be seen, the proposed method outperforms the INS-aided tight CP, tight CP, and the DGPS. To compare the performance[16], we defined $(1-ErrorB/ErrorA)\times 100\%$ as the demonstrate of the percentage of improvement achieved better than method A with the using of method B. And any error indicators type will be ok with Error A and Error B, such as accuracy, precision, and rmse. It is summarized in Table 3 that the improvements of the performance with different methods in the simulation dense urban scenarios. As can be seen, up to 23%, 26%, and 33% improvement, in terms of rmse, were achieved over the INS-aided tight CP, the tight CP and DGPS, respectively.

Table 2. Experimental Results for Relative Positioning Errors in Dense Urban Scenarios

Methods	rmse (m)	accuracy(m)	precision(m)
T-CP with IMU (proposed)	2.91	1.51	2.49
INS-aided T-CP [17]	3.77	1.63	3.40
T-CP [16]	3.93	1.72	3.54
DGPS [7]	4.36	1.83	4.02

Table 3. Percentage of Improvements Achieved by the Proposed Method over other Existing Methods in Dense Urban Scenarios

Methods	rmse	accuracy	precision
Proposed method over T-CP with INS	23%	7%	27%
Proposed method over T-CP	26%	12%	30%
Proposed method over DGPS	33%	17%	38%

To further evaluate the performance of proposed method in extremely abominable urban environment as GPS complete outage scenario, the GPS data are completely mask four times in the 14-minute data log. That is, beginning at 100s, 300s, 500s, and 700s, the GPS measurements of all satellites were made unavailable, i.e. 100% break off. The duration of the GPS breakoff was between 1s to 20s (instead of 1s to 10s in [17]) to satisfy a more general urban environment.

Fig. 5-7 shows the accuracy, precision and rmse as a function of satellite break off time for many different techniques. Just as expected, the errors in precision and accuracy and rmse growth considerably together with increased GPS outage duration, and the low-cost IMU tight CP method proposed in this paper outperforms all three other methods. It can also be seen that the performance of the INS-aided tight CP method [17] declines faster than the three other methods when the duration of GPS outage exceeds 12 seconds. The most noteworthy result from Fig.5-7 is that the proposed method produces the smallest errors for all GPS outage durations.

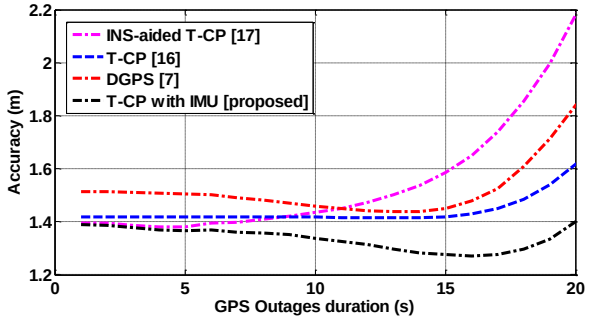

Figure 5. Accuracy of Different Techniques over GPS Outage Periods

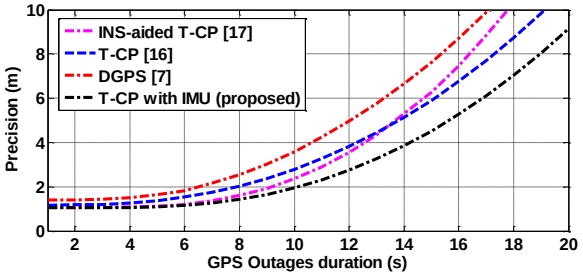

Figure 6. Precision of Different Techniques over GPS Outage Periods

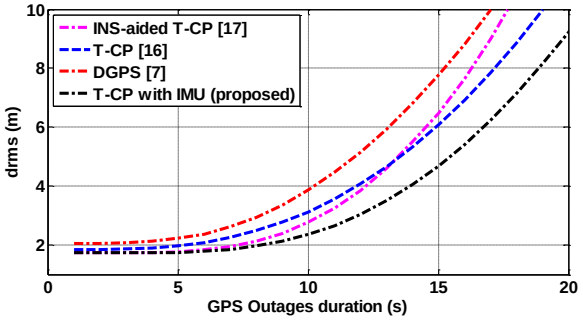

Figure 7. rmse of Different Techniques over GPS Outage Periods

For a better visualization of performance improvement, Fig. 8 shows the rmse improvement achieved as a function of GPS outage duration. It can be noticed, while the GPS break off duration, up to 35%, 45%, and 54% improvement were achieved over the INS-aided tight CP method, the tight CP method and DGPS, respectively. It is also evident that the degree of improvement delivered by the proposed technique upon the other techniques is consistent and becomes more significant as the GPS outage duration increases.

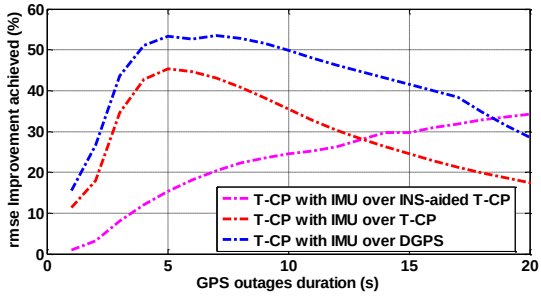

Figure 8. Improvement Achieved over GPS Outage Periods

5. Conclusion

A CP method has been proposed to improve the performance of relative positioning for the dense urban environment, which is based on fusing GPS pseudoranges and Doppler shifts and accelerations of the vehicles. Compared with the previous INS-aided tight CP, the tight CP and DGPS, the proposed method has up to 23%, 26%, and 33% rmse improvement respectively in the simulation dense urban scenario. Moreover, in the extremely abominable environment, GPS completely unavailable scenario, up to 35%, 45%, and 54% improvement can be achieved when compared against the INS-aided tight CP, the tight CP and DGPS, respectively.

It is noteworthy that there are still gaps between our available results and practical

safety-critical applications , for instance , avoiding the collision during the GPS break off time. But, radars, digital maps, odometer, and cameras can also be used represent future work.

Acknowledgment

We want to thank Dr. N. Alam from Caterpillar Trimble Control Technologies, Dayton, OH USA, because of his help. We also would like to thank A/Prof. A. Kealy from the Department of Infrastructure Engineering, University of Melbourne, Parkville, Australia, Dr. C. Hill and S. Ince from the Nottingham Geospatial Institute, University of Nottingham, Nottingham, U.K., and because of their support and our collaboration we done this work very well. Meanwhile, this work was supported by National Nature Science Foundation of China under grants 61102107 and 61374208, and by the China Fundamental Research Funds for the Central Universities under grants HEUCFX41310.

References

[1] "Vehicle Positioning for C-ITS in Australia", Austroads Research Report, https://www.onlinepublications.austroads.com.au/items/AP-R431-13.
[2] R. Tatchikou, S. Biswas and F. Dion, "Cooperative vehicle collision avoidance using inter-vehicle packet forwarding", Proc. IEEE GLOBECOM Conf, **(2005)**.
[3] H. Wymeersch, "Cooperative localization in wireless networks", Proceedings of the IEEE, **(2009)**.
[4] A. Boukerche, "Vehicular Ad Hoc Networks: A New Challenge for Localization-Based Systems", Computer Communications, vol. 31, **(2008)**, pp. 2838-2849.
[5] N. Patwari, J. N. Ash, S. Kyperountas, A. O. Hero, R. L. Moses and N. S. Correal, "Locating the nodes: cooperative localization in wireless sensor networks", IEEE Signal Processing Magazine, vol. 22, no. 4, **(2005)**, pp. 54–69.
[6] E. D. Kaplan and C. J. Hegarty, "Understanding GPS Principles and Applications", 2nd ed. Norwood, MA, USA: Artech House, **(2006)**.
[7] C. R. I. Jock, P. Y. Ko, A. Hansen, D. H. Dai, S. Pullen, B. S. Pervan and B. W. Parkinson, "The Effects of Local Ionospheric Decorrelation on LAAS: Theory and Experimental Results", In ION NTM, **(1999)**.
[8] B. H. Wellenhof, H. Lichtenegger and J. Collins, "Global Positioning System Theory and Practice", 5th ed. New York, NY, USA: Springer-Verlag, **(2001)**.
[9] R. Parker and S. Valaee, "Vehicular node localization using receivedsignal-strength indicator", IEEE Trans. Veh. Technol., vol. 56, no. 6, **(2007)**, pp. 3371–3380.
[10] N. Patwari, A. O. Hero, M. Perkins, N. S. Correal and R. J. O'Dea, "Relative location estimation in wireless sensor networks", IEEE Trans.Signal Process., vol. 51, no. 8, **(2003)**, pp. 2137–2148.
[11] S. Venkatraman, J. Caffery and H. R. You, "Location Using LOS Range Estimation in NLOS Environments", IEEE VTC Spring, Birmingham, AL, **(2002)**, pp. 856-860.
[12] N. Alam, A. T. Balaie and A. G. Dempster, "Dynamic path loss exponent and distance estimation in a vehicular network using Doppler effect and received signal strength", Proc. IEEE VTC—Fall, **(2010)**; Ottawa, ON, Canada.
[13] E. Richter, "Cooperative relative localization using vehicle-to-vehicle communications", 12th International Conference on Information Fusion, **(2009)**; Seattle, WA.
[14] T. S. Dao, "Markov-based lane positioning using intervehicle communication", IEEE Transactions on Intelligent Transportation Systems, vol. 8, **(2007)**, pp. 641-650.
[15] N. Alam, A. T. Balaei and A. G. Dempster, "Range and range-rate measurements using DSRC: Facts and challenges", Presented at the Int. GlobalNavigation Satellite Systems (IGNSS) Symp., **(2009)**; Surfers Paradise, Australia.
[16] N. Alam, A. T. Balaei and A. G. Dempster, "Relative positioning enhancement in VANETs, a tight integration approach", IEEE Trans. Intell. Transp. Syst., vol. 14, no. 1, **(2013)**, pp. 47–55.
[17] N. Alam, A. Kealy and A. G. Dempster, "An INS-aided tight integration Approach for Relative Positioning Enhancement in VANETs", IEEE Trans. Intell. Transp. Syst., vol. 14, no. 4, **(2013)**, pp. 1992–1996.
[18] W. J. Lei, S. C. L and J. Chen, "A Fountain Transmission Scheme for Inter- vehicle Safety MessageTransmission and Analysis of the Optimal Hop Number", Journal of Harbin University of Science and Technology, vol. 5, no. 3, **(2013)**, pp. 70–75.
[19] S. P. Teasley, W. M. Hoover and C. R. Johnson, "Differential GPS navigation", Presented at the IEEE PLANS, Position Location Navigation Symp., **(1980)**; Atlantic City, NJ, USA.
[20] D. H. Titterton and J. L. Weston, "Strapdown inertial navigation technology", Peter Pergrinus Ltd., **(1997)**.

[21] G. Dissanayake, S. Sukkarieh, E. Nebot and H. D. Whyte, “The aiding of a low-cost strapdown inertial measurement unit using vehicle model constraints for land vehicle applications", IEEE Trans. Robot. Autom., vol. 17, no. 5, **(2001)**, pp. 731–747.
[22] L. H. Ma, K. L. Wang and M. Shao, “Initial alignment on moving base using GPS measurements to construct new vectors", Measurement, vol. 46, no. 3, **(2013)**, pp. 2405–2410.
[23] P. D. Groves, "Principle Of GNSS, Inertial, and Multisensor Integrated Navigation Systems", Artech House, Boston, **(2008)**.
[24] M. S. Grewal and A. P. Andrews, "Kalman Filtering Theory and Practice", Prentice-Hall, **(1993)**.
[25] ETSI, "Road Transport and Traffic Telematics (RTTT); Dedicated Short Range Communication (DSRC) transmission equipment (500 kbit/s / 250 kbit/s) operating in the 5,8 GHz Industrial, Scientific and Medical (ISM) band; Part 1: General characteristics and test methods for Road Side Units (RSU) and On-Board Units (OBU)", ed: European Telecommunications Standards Institute, vol. EN 300 674-1, **(2004)**.
[26] J. Chao, Y. Q. Chen, W. Chen, Z. Ding, N. Wong and M. Yu, “An experimental investigation into the performance of GPS-based vehicle positioning in very dense urban areas", J. Geospatial Eng., vol. 3, **(2001)**, pp. 59–66.

